

## Starch-capped silver oxide (Ag<sub>2</sub>O) nanoparticles: synthesis, characterization and antibacterial activity

P. N. Mahlambi<sup>a</sup>, M. J. Moloto<sup>b,\*</sup>

<sup>a</sup>University of KwaZulu Natal, Department of Chemistry, Private Bag X021, Scottsville, 3209, South Africa, South Africa

<sup>b</sup>Institute for Nanotechnology and Water Sustainability, College of Science, Engineering and Technology, University of South Africa, Florida Park, Roodeport, 1709, South Africa

Silver oxide nanoparticles were synthesized at room temperature using a green synthetic method and water as a solvent. Starch was used as a capping and reducing agent because it is cheap, non-toxic and environmentally friendly. The effect of precursor and capping agent concentrations were investigated. The nanoparticles have been characterized using spectroscopic and morphological techniques. The spectrum of Ag<sub>2</sub>O nanoparticles showed the maximum absorbance range at 350-366 nm. TEM analysis showed a size particle range of 2-14 nm. The increase in precursor concentration showed an increase in particle size while increasing the capping agent concentration resulting in reduced particle size. Increased capping concentration also resulted in the change to nanofibers. The nanoparticles showed antibacterial activities against both *Staphylococcus aureus* and *Escherichia coli* strains. The 2:1 Ag<sub>2</sub>O ratio showed the best activity towards both strains,  $15 \pm 0.19$  and  $14 \pm 0.11$  mm diameter, respectively.

(Received March 7, 2022; Accepted 17, 2022)

**Keywords:** Silver oxide, Nanoparticles, Starch, Capping agents, Antibacterial activity

### 1. Introduction

Antibacterial agents are vital to fighting infectious diseases. However, due to the wide use of antibacterial agents, most bacterial species have developed resistance to antibacterial drugs, which is a significant problem [1]. Thus, the need to develop alternative approaches to treat bacterial diseases has been encouraged and investigated. Among these methods, the use of nanoscale materials (nanoparticles) has appeared to be the novel antimicrobial agents and have proven their potential efficiency to treat infectious diseases, which include antibiotic-resistant ones, both in vitro and in animal models [2]. Nanoparticles offer improved properties compared to classical organic antibacterial agents due to their high surface area to volume ratio, generating new mechanical, chemical, electrical, optical, magnetic, electro-optical and magneto-optical properties [3]. Silver nanoparticles are reported with more excellent antimicrobial properties than other metal nanoparticles due to the exceptional large surface area that offers better contact with microorganisms.

In this work, the synthesis of starch capped Ag<sub>2</sub>O nanoparticles is reported. The nanoparticles have been prepared at room temperature using starch as a capping and a stabilizing agent, and water has been used as a solvent, a form of Green Chemistry. This has been undertaken because there has been an increasing need to develop low cost, non-toxic and environmentally friendly procedures [4]. Starch has been used because it is environmentally friendly, biocompatible, and easily modified for a wide range of potential applications. The emergence of antibiotic and multidrug-resistant of bacteria is known as a critical challenge for public health. The killing of antibiotic-resistant bacteria needs multiple expensive drugs that may also have side effects. Due to this, treatments are expensive and require more time. Nanoparticles promise to offer a new strategy to attack multidrug-resistant bacteria [5]. For this reason, the antibacterial

---

\* Corresponding author: molotmj@unisa.ac.za  
<https://doi.org/10.15251/DJNB.2022.173.921>

properties of the synthesized Ag<sub>2</sub>O nanoparticles have been investigated using Gram-negative (*Escherichia coli*) and Gram-positive (*Staphylococcus aureus*) bacteria.

## 2. Experimental

### 2.1. Chemicals

Sodium hydroxide (NaOH) (99.9%), silver nitrate (AgNO<sub>3</sub>) (99.8%) and, soluble starch (99.9%) were purchased from Merck (Germany). Acetone (99.8%) was purchased from Sigma Aldrich. Muller-Hinton broth and Muller-Hinton agar were purchased from Neogen (Michigan). *Escherichia coli* and *Staphylococcus aureus* bacterial cells were bought from the supplier Anatech (South Africa). All chemicals were used as purchased without any further purification.

### 2.2. Synthesis of starch capped Ag<sub>2</sub>O nanoparticles

Starch capped silver oxide nanoparticles were prepared at room temperature. Silver nitrate solution (20 mL, 0.1 M) was added to different amount of starch (0.5-2 % (w/v)) in a round-bottom flask while stirring. Sodium hydroxide solution (20 mL, 0.1 M) was then added to the reaction mixture. This was further stirred for 2 hours at room temperature. The resultant solution was centrifuged and extracted with acetone to obtain a precipitate of Ag<sub>2</sub>O nanoparticles. It was then dried at room temperature and characterized.

### 2.3. Characterization techniques

A Perkin Elmer Lambda 25 UV-Vis spectrophotometer was used to carry out all-optical studies. The measurements were performed at 200-1100 nm wavelength range at room temperature. Fourier transform infrared (FT-IR) analyses using a Perkin Elmer spectrum 400 FT-IR-NIR Spectrometer equipped with a universal ATR sampling accessory. The structure of the nanoparticles was studied using a JEOL JEM-2100 transmission electron microscope operating at 200 kV. The TEM has coupled with a dispersive energy X-ray (EDX) detector used to determine the elemental composition of the synthesized nanoparticles. The X-ray diffraction patterns were recorded by a Bruker D2 diffractometer at 40 kV and 50 mA. Secondary graphite monochromated Co K alpha radiation ( $\lambda = 1.7902 \text{ \AA}$ ) was used, and the measurements were taken at high angle  $2\theta$  in a range of 5°-90° with a scan speed of 0.01°  $2\theta \text{ s}^{-1}$ . For thermal analysis, a PerkinElmer Thermogravimetric Analyzer (TGA 4000) was used. The samples were heated under nitrogen, and the heating range was between 25 and 900 °C at a heating rate of 5°/min.

### 2.4. Antibacterial activity of Ag<sub>2</sub>O nanoparticles

The antibacterial activity of the selected nanoparticles was performed by using the disc diffusion method. About 20 mL of sterile molten Mueller Hinton agar was poured into sterile petriplates. Triplicate plates were swabbed with the overnight culture ( $10^5$  cells/mL) of *Escherichia coli* and *Staphylococcus aureus* bacteria. The starch capped Ag<sub>2</sub>O nanoparticle samples with different concentrations (6.0, 3.0, 1.5, 0.75, 0.37 mg/mL) were added into different discs, placed in the Petri plates and incubated for 24 hours at  $37 \pm 2^\circ\text{C}$ . After 24 hours of incubation, the zone of inhibition was measured and expressed as a millimetre in diameter. The 96 well Microtitre Dilution Assay method by Chillar et al. [6] was used to investigate the minimum inhibitory concentration (MIC) of the nanoparticles. Amoxicillin was used as a positive control. The MIC was evaluated using (0.37, 0.18, 0.093, 0.046, 0.023 mg/mL) concentrations of nanoparticles. All the experiments were performed in triplicates.

### 2.5. Determination of the growth curves of bacterial cells exposed to silver oxide nanoparticles

To study the growth curves of *Escherichia coli* and *Staphylococcus aureus* bacterial cells, exposed Mueller-Hinton broth with 3 mg/mL of nanoparticles was used. The concentration of the bacterial cells was adjusted to  $10^5$  CFU/mL. Each culture was then incubated in a shaking incubator at 37°C for 24 h. Growth curves of bacterial cell cultures were attained through repeated measures (every four hours) of the optical density (O.D.) at 600 nm.

### 3. Results and discussion

The effect of starch capping agent concentration on the size and shape of the synthesized nanoparticles was investigated using different starch concentrations (0.5, 1.0 and 2.0 % (w/v)). The concentration of the precursor was kept constant at 1:1 silver nitrate salt and sodium hydroxide ratios. The effect of capping agent concentration was investigated since it has a role of binding to the surface of the nanoparticles, thus preventing agglomeration. This then leads to better dispersion and uniform-sized nanoparticles. Precursor concentration was investigated using different concentration ratios of silver nitrate salt and sodium hydroxide ratios (1:1, 1:2 and 2:1), while keeping the starch concentration constant at 1.0 % (w/v). The precursor concentration variation was investigated for its influence on the size and shape of the nanoparticles.

#### 3.1. Optical analysis

Fig. 1A shows the absorption spectra for the effect of starch capping agent concentration on optical properties of  $\text{Ag}_2\text{O}$  nanoparticles. The maximum absorption peak was observed at 361 nm (3.43 eV) for 0.5 % (w/v) of starch, 350 nm (3.54 eV) for 1.0 % (w/v), 366 nm (3.38 eV) for 2.0% (w/v). The 1.0 % (w/v) starch capped nanoparticles gave a sharp peak indicating the small spherical nanoparticles formed. A broad peak was observed for the 2.0 % (w/v) starch capped nanoparticles, confirming nanofibers' formation. The increase in peak absorption intensity and the shift towards lower wavelength with an increase in capping agent concentration (0.5 % (w/v) - 1.0 % (w/v)) was a result of the formation of increased small-sized and well-dispersed nanoparticles. This was further confirmed by the TEM results (Fig. 2). Fig. 1B shows the absorption spectra for the effect of precursor concentration. The absorption shoulder appeared at 350 nm (3.54 eV) for (1:1), 355 nm (3.49 eV) for 1:2, 354 nm (3.50 eV) for 2:1 precursor concentration ratio. The decrease in the absorbance peak with an increase in precursor concentration might indicate the presence of silver oxide (not reduced), which might be due to the concentration of dissolved starch being insufficient to reduce all the present concentrations of the silver ions [7]. The results obtained in this study also agree with studies on precursor concentrations as reported by Mayekar J et al. [8].

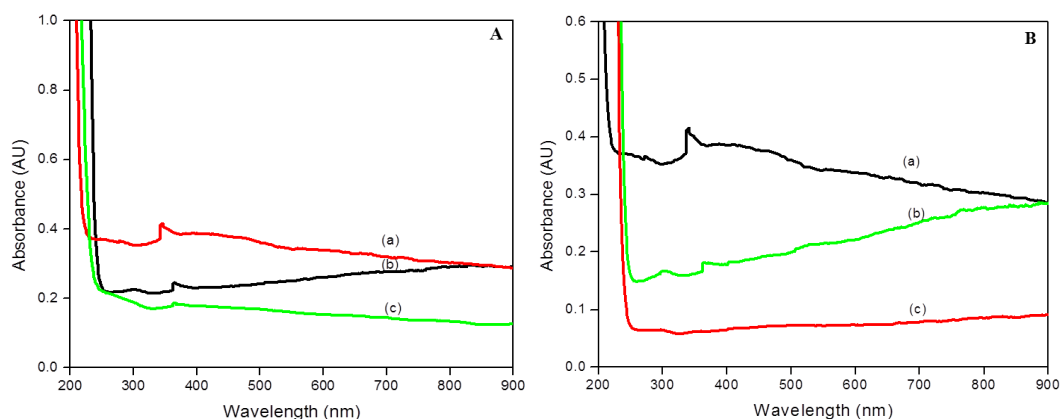


Fig. 1. A UV-Vis spectra for starch capped  $\text{Ag}_2\text{O}$  nanoparticles with a) 1.0 % (w/v), b) 0.5 % (w/v) and c) 2.0 % (w/v) starch. and Fig. 1B UV-Vis spectra for starch capped  $\text{Ag}_2\text{O}$ , a) 1:1, b) 2:1 and c) 1:2 precursor mole ratios.

#### 3.2. TEM analysis

Fig. 2 shows the micrographs and histograms for the effect of starch capping agent concentrations (0.5, 1.0 and 2.0 % (w/v)) on the size and shape of  $\text{Ag}_2\text{O}$  nanoparticles. A smaller percentage (0.5 % (w/v)) of capping agent yielded irregular and aggregated particles with an average diameter of 11.31 nm. The smaller quantity of nanoparticles is due to the inefficient and smaller amount of capping agent that controls the growth and aggregation of nanoparticles, thus forming larger particles. Well dispersed, spherically shaped nanoparticles with a diameter of 2.00

nm were observed at 1.0 % (w/v). This means that the amount of capping agent used could provide stable surface passivation resulting in protection and prevention of the aggregation of particles. A decrease in nanoparticle size with an increase in capping agent concentration was observed from 0.5 % (w/v) to 1.0 % (w/v) starch. This could be because the reaction was faster and was strongly influenced by the number of nuclei formed at a given time, which favoured autolytic growth and thus gave rise to a large number of small nanoparticles [9]. These results agree with those reported by Shen X.S et al., Li CC et al. [10, 11]. For 2.0 % (w/v) starch, nanofibers with a mean diameter of 14.96 nm were obtained. This can be attributed to an increased amount of starch interacting with the nanoparticle's surface, resulting in a change in shape. This could also mean that growth by ripening took place, nucleation and growth occurred simultaneously and thus led to the formation of fibre-like structures [12]. Varying the capping agent ratio to precursor ratio has been reported to have changed particle morphology in some systems due to varying ability to stabilize certain planes. Capping agents are used to decrease the surface energies of crystals, thus controlling the crystal growth. The capping agent selectively binds to the different crystallographic faces so that the shape of nanocrystals can be controlled by the capping agent [13].

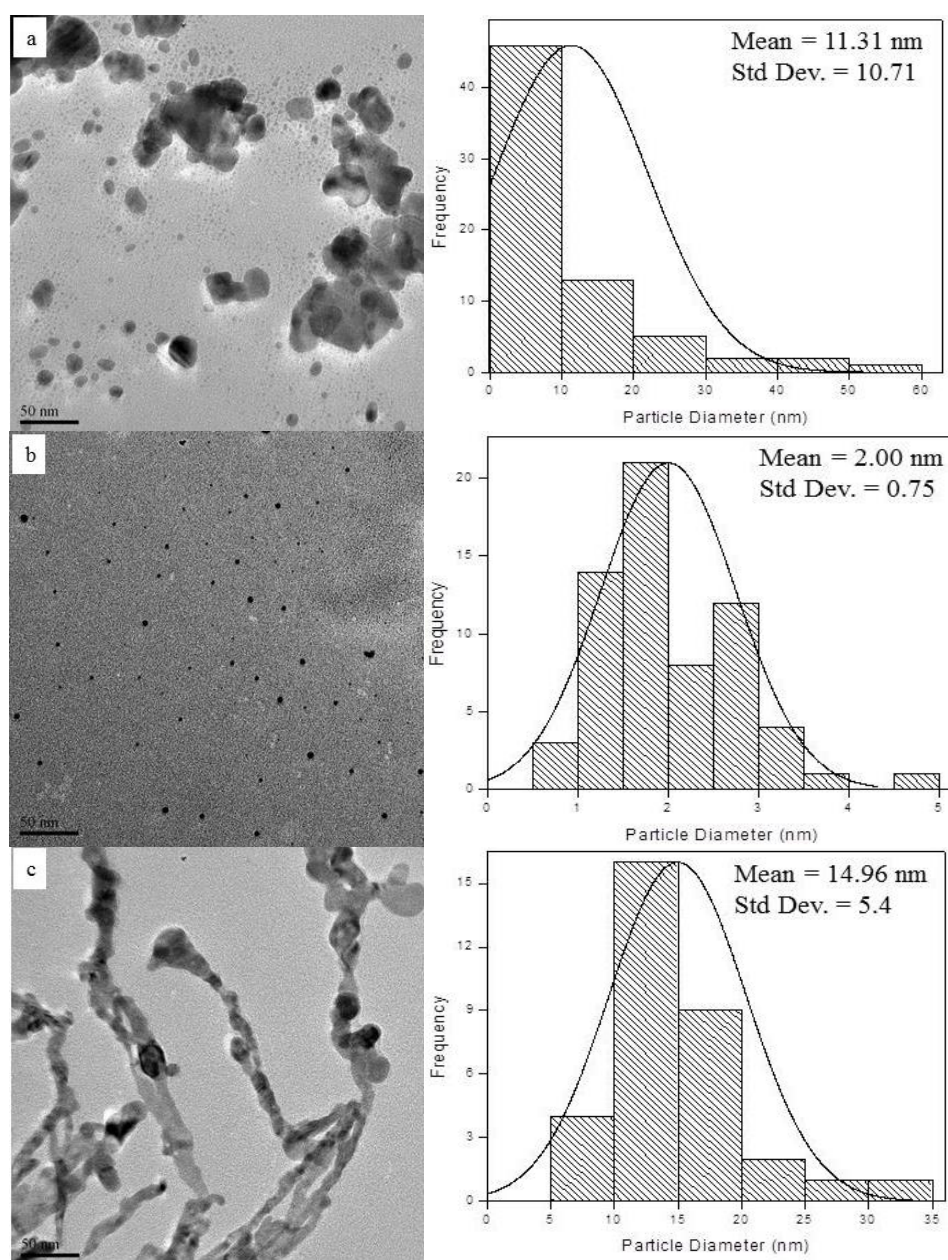


Fig. 2. TEM image and size histograms for starch capped  $\text{Ag}_2\text{O}$  (1:1) nanoparticles with a) 0.5 % (w/v), b) 1.0 % (w/v), c) 2.0 % (w/v) starch.

Fig. 3 shows the micrographs and histograms for the effect of precursor concentrations (1:1, 1:2 and 2:1) on the size and shape  $\text{Ag}_2\text{O}$  nanoparticles. The TEM results obtained showed well-dispersed nanoparticles with spherical morphology for all precursor concentrations studied. It was observed that the nanoparticle size increased with an increase in precursor concentration. Similar behaviour was reported by Hebeish A et al.[7] and Song HY et al.[14]. The result for the increase in particle size might have arisen from the same 1.0 % (w/v) of starch used for the variation of the concentration, which led to insufficient and less effective to passivate nanoparticles at higher precursor concentrations. The particle sizes as calculated are 2.00 nm (1:1), 4.16 nm (1:2), 3.72 nm (2:1) ratios. The ratio 1:1 gave nanoparticles with better monodispersity. Elemental analysis by EDX indicated the presence of Ag and O in the ratio 2 to 1, which is in good agreement with the theoretical formula of the compound.

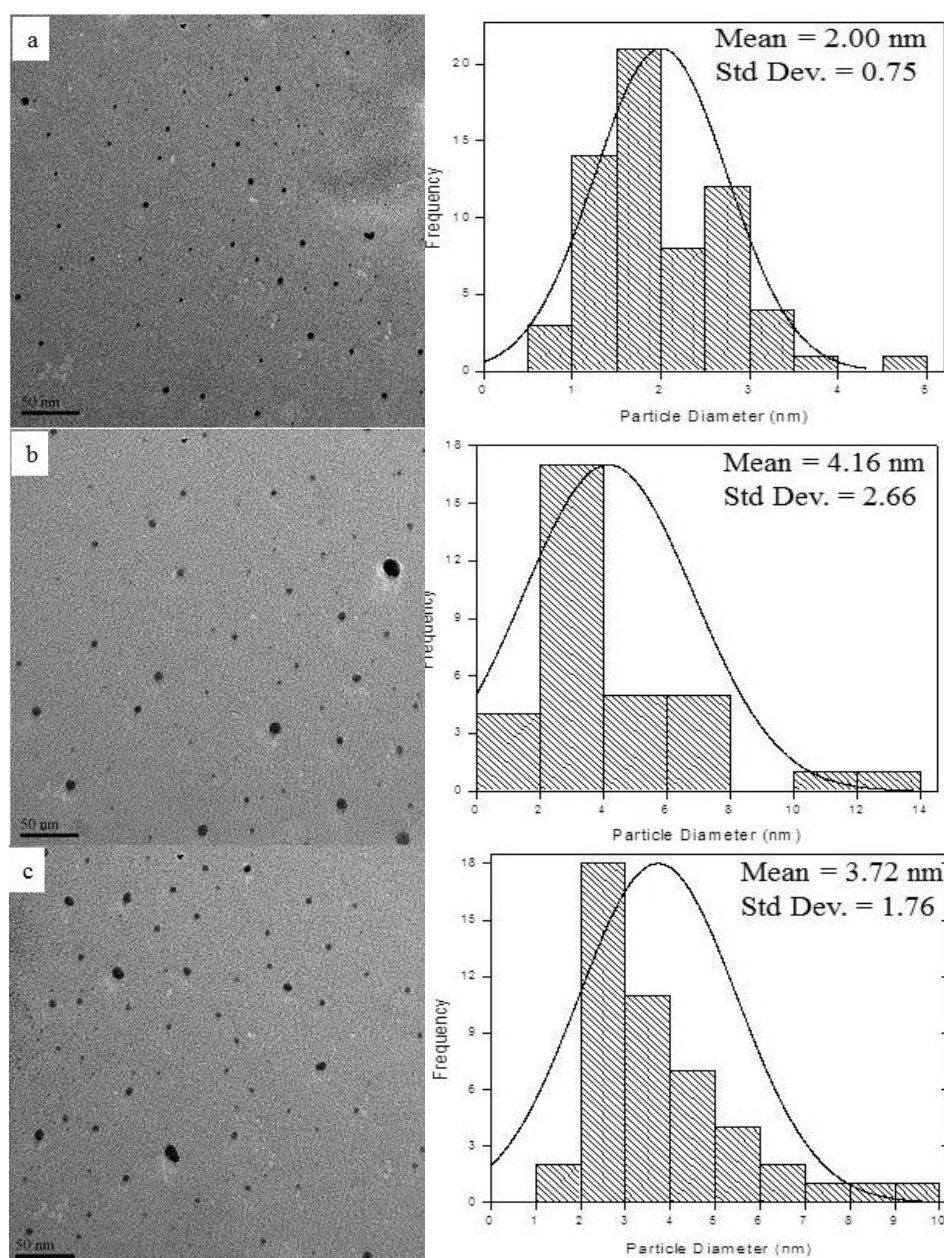


Fig. 3. TEM images for starch capped  $\text{Ag}_2\text{O}$  nanoparticles with 1.0 % (w/v) starch a) 1:1, b) 1:2, c) 2:1.

### 3.3. FT-IR spectral analysis

FT-IR spectroscopy was used to investigate the surface interaction of the synthesized nanoparticles with the capping agent. Fig. 4 shows the IR spectra of starch capped  $\text{Ag}_2\text{O}$  nanoparticles at different precursor concentrations. A strong band observed at  $3305\text{ cm}^{-1}$  was attributed to the O-H stretching of starch. Its width was attributed to the formation of inter and intramolecular hydrogen bonds. At  $2926\text{ cm}^{-1}$ , an asymmetric stretching of C-H band was observed, while the band at  $1647\text{ cm}^{-1}$  was attributed to water adsorbed in the amorphous region of starch. The characteristic band at  $1085\text{ cm}^{-1}$  was attributed to C-O-H bending of starch. The shift at  $3305$  and  $1085\text{ cm}^{-1}$  band to  $3285$  and  $1079\text{ cm}^{-1}$ , respectively, was observed in the presence of nanoparticles. This might be due to inter and intramolecular interaction of nanoparticles with starch. The O-H band was broader in the starch capped nanoparticles as compared to starch alone. These observations show the interaction of  $\text{Ag}_2\text{O}$  nanoparticles with the hydroxyl group of starch [7, 15].

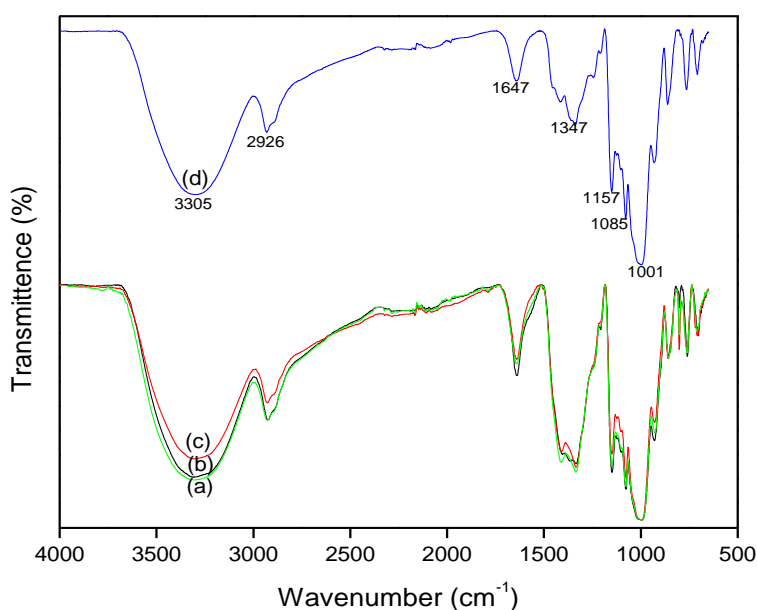


Fig. 4. FTIR spectra of starch capped  $\text{Ag}_2\text{O}$  nanoparticles with 1.0 % (w/v) starch, a) 2:1, b) 1:1, c) 1:2 precursor mole ratios and d) pure starch.

### 3.4. XRD Analysis

The phase identification of the synthesized nanoparticles was obtained using XRD technique. The XRD patterns of starch capped  $\text{Ag}_2\text{O}$  (1:1) nanoparticles are shown in Fig. 5. The graph shows broad peaks, confirming small particle size as observed from TEM results (Fig. 3). The  $\text{Ag}_2\text{O}$  nanoparticles pattern can be indexed to cubic phase (JCPDS card 03-065-3289), with 200 ( $44.5^\circ$ ) planes of  $\text{Ag}_2\text{O}$  distinguishable in the pattern.

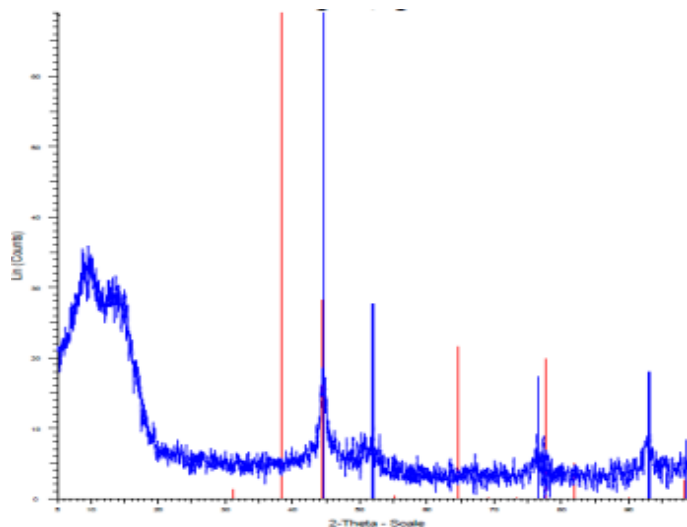


Fig. 5. XRD patterns of starch capped  $\text{Ag}_2\text{O}$  nanoparticles with 1.0 % (w/v) starch.

### 3.5. TGA Analysis

The thermal analysis of the synthesized nanoparticles was investigated using TGA technique. The TGA thermograms of the starch capped  $\text{Ag}_2\text{O}$  nanoparticles is shown in Fig. 6. The first degradation step observed at around 100 °C was due to the desorption of water from the nanoparticles. The weight loss due to starch degradation was observed at 317 °C for 1:1 ratio, 300 °C for 1:2 ratio and 319 °C for 2:1 ratio.

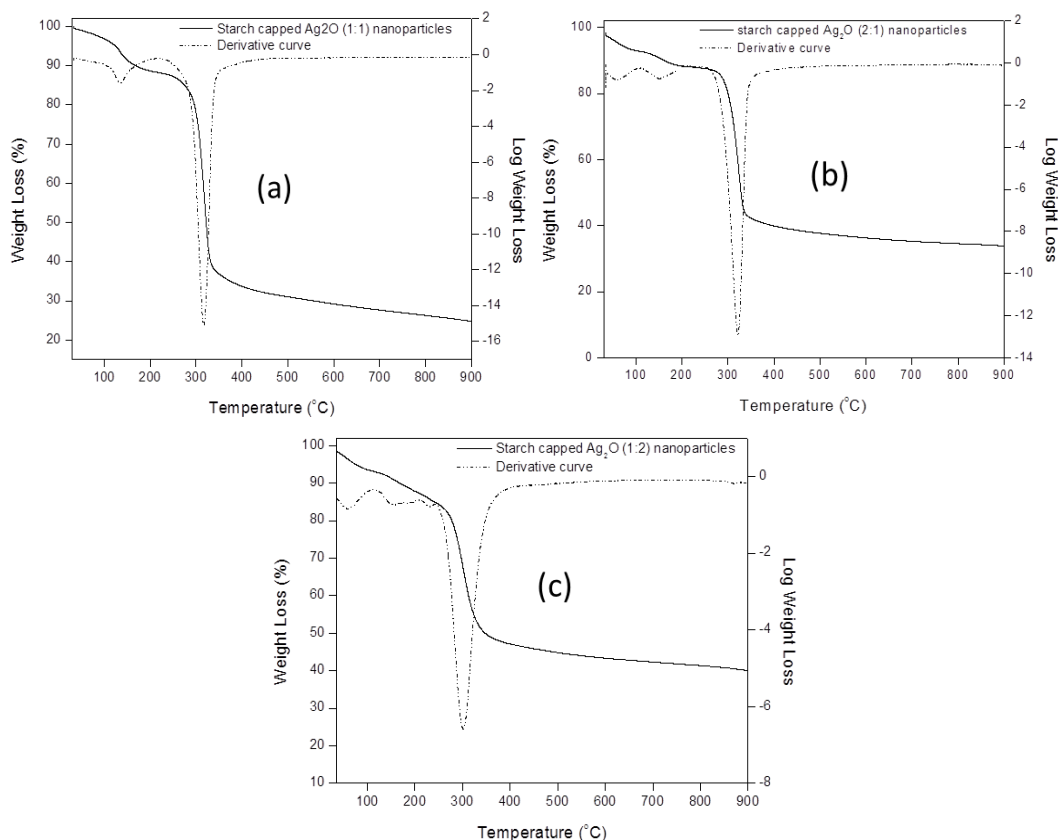


Fig. 6. TGA and derivatives thermographs of starch capped  $\text{Ag}_2\text{O}$  nanoparticles with 1.0 % (w/v) starch, a) 1:1, b) 1:2, c) 2:1.

This means that the mass ratios influenced the stability of the starch capped nanoparticles. No further weight loss was observed, indicating a complete degradation of starch and that the remaining silver oxide was stable up to temperatures around 900 °C.

### 3.6. Antibacterial Activity

The antibacterial activity of different concentrations (6.0-0.37 mg/mL) of silver oxide nanoparticles was evaluated using *Escherichia coli* and *Staphylococcus aureus*. The results obtained for the antibacterial studies are shown in Table 1. The synthesized nanoparticles showed a positive response towards both bacterial species in all concentrations studied. The minimum inhibitory concentration (MIC) was then further investigated using 0.37-0.023 mg/mL of nanoparticles; the results are shown in Table 2. Ag<sub>2</sub>O nanoparticles showed a maximum inhibition zone of 15 ± 0.19 mm diameter against *Staphylococcus aureus*, while they showed a maximum inhibition zone of 14 ± 0.11 mm diameter for *Escherichia coli*. The inhibition zones observed in all precursor concentration ratios are comparable, which means that the bacterial activity is independent of precursor concentration ratios. The reason for this could be the similarity in shape and size of the nanoparticles synthesized in all precursor ratios. From the MIC results, the Ag<sub>2</sub>O nanoparticles showed the minimum inhibition at a concentration of 0.023 mg/mL against *Escherichia coli* for the 1:1 and the 1:2 precursor ratios. However, throughout the investigated concentrations and in all precursor ratios, no minimum inhibitory concentration was observed for *Staphylococcus aureus*. This means that the nanoparticles are more sensitive towards *Staphylococcus aureus* than *Escherichia coli*. Results indicate that the prepared Ag<sub>2</sub>O nanoparticles are susceptible to gram-negative and gram-positive bacterial strains. The activity observed from the metal nanoparticles is due to the nanoparticles carrying positive charges and the microbes having negative charges. This results in some electromagnetic attraction between the nanoparticles and the microbes. When the attraction takes place, the microbes get oxidized and die instantly. In general, the nanomaterials release ions that react with the thiol groups (-SH) of the proteins present on the bacterial cell surface, which leads to cell lysis [16].

Table 1. Antibacterial activity of nanoparticles against bacteria.

Nanoparticles	Concentration (mg/mL)	Zone inhibition (mm)	
		<i>Escherichia. Coli</i>	<i>Staphylococcus aureus</i>
<b>1:1 Ag<sub>2</sub>O</b>	6.0	11 ± 0.21	14 ± 0.28
	3.0	11 ± 0.36	11 ± 0.24
	1.5	11 ± 0.14	11 ± 0.33
	0.75	11 ± 0.33	11 ± 0.34
	0.37	10 ± 0.23	10 ± 0.25
<b>1:2 Ag<sub>2</sub>O</b>	6.0	12 ± 0.25	13 ± 0.34
	3.0	12 ± 0.16	13 ± 0.15
	1.5	12 ± 0.19	13 ± 0.22
	0.75	11 ± 0.14	13 ± 0.39
	0.37	9 ± 0.32	12 ± 0.34
<b>2:1 Ag<sub>2</sub>O</b>	6.0	14 ± 0.11	15 ± 0.19
	3.0	12 ± 0.24	15 ± 0.11
	1.5	12 ± 0.17	15 ± 0.29
	0.75	12 ± 0.13	14 ± 0.16
	0.37	12 ± 0.19	13 ± 0.19

Table 2. MIC of nanoparticles against bacteria.

Nanoparticles	Concentration (mg/mL)	
	<i>Escherichia coli</i>	<i>Staphylococcus aureus</i>
1:1 Ag <sub>2</sub> O	0.023	-
1:2 Ag <sub>2</sub> O	0.023	-
2:1 Ag <sub>2</sub> O	-	-

(-) means no minimum inhibitory concentration was found throughout the concentrations used.

### 3.7. Growth curves of bacterial cells treated with Ag<sub>2</sub>O nanoparticles

The bacterial growth of *Escherichia coli* and *Staphylococcus aureus* cells treated with nanoparticles is lower than those in the control group (Fig. 7a-d). This means that Ag<sub>2</sub>O nanoparticles can hinder the growth and the replication of bacterial cells. Both bacterial cells showed an increase in growth from 0 to 8 hours which means that the bacteria growth inhibition of these nanoparticles is time-dependent. *Staphylococcus aureus* cells treated with nanoparticles were then stable from 8 to 24 hours (Fig. 7c). *Escherichia coli* cells treated with nanoparticles showed a decrease in growth from 8 to 16 hours and then stabilized from 16 to 24 hours (Fig. 7d).

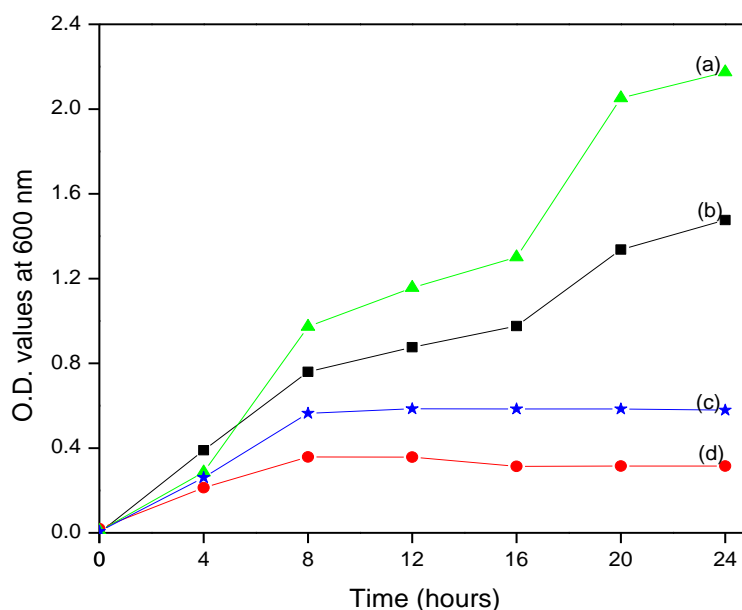


Fig. 7. Growth curves of a) *Staphylococcus aureus* alone, b) *Escherichia coli* alone, c) *Staphylococcus aureus* with Ag<sub>2</sub>O nanoparticles, d) *Escherichia coli* with Ag<sub>2</sub>O nanoparticles.

## 4. Conclusion

From the results obtained, it can be concluded that starch capped Ag<sub>2</sub>O nanoparticles were successfully synthesized in a cubic phase. Increasing the capping agent concentration showed a decrease in nanoparticle size; however, a further increase resulted in a shape change from spherical to fibre structured shape. The increase in precursor concentration showed a slight increase in nanoparticle size, and there was no change in shape. These findings indicated that the capping agent affects both the size and shape of nanoparticles, while the precursor concentration influenced only the size of nanoparticles. It can be concluded from the present study that the Ag<sub>2</sub>O nanoparticles could be used as an effective antibacterial agent for the management of bacteria. The

antibacterial activity showed to be independent of the precursor concentration ratios as it gave comparable inhibition results in all precursor ratios. On the other hand, the bacteria growth inhibition showed to be time-dependent.

## References

- [1] Witte W, *J. Infect. Genet. Evol* 4(3), 187-191 (2004); <https://doi.org/10.1016/j.meegid.2003.12.005>
- [2] Huh A.J, Kwon Y.J., *J. Control. Release* 156, 128-145 (2011); <https://doi.org/10.1016/j.jconrel.2011.07.002>
- [3] Xia Y., *Nat. Mater* 7, 758-760 (2008); <https://doi.org/10.1038/nmat2277>
- [4] Emilio I., Alarcon K., Udekwu M., Skog M.L., Pacion K.G., Stamplecoskie M., *Biomater* 33(19), 4947-4956 (2012); <https://doi.org/10.1016/j.biomaterials.2012.03.033>
- [5] Hajipour M.J., Fromm K.M., Ashkarran A.K., de Aberasturi D.J., de Larramendi I.R., Rojo F., Serpooshan V., Parak W.J., Mahmoudi M., *Trends Biotechnol* 30, 499-511 (2012); <https://doi.org/10.1016/j.tibtech.2012.06.004>
- [6] Chhillar A., Gahlaut A., Evaluation of Antibacterial potential extract using resazurin based microtiter dilution assay, (2013), *Int. J. Pharm. and Pharm. Sci.* 5(2), 372-376.
- [7] Hebeish A., El-Rafie M.A., El-Sheikh M.A., El-Naggar M.E., *J. Nanotech.* 2013, 1; <https://doi.org/10.1155/2013/201057>
- [8] Mayekar J., Dhar V., Radha S., Role of salt precursor in the synthesis of zinc oxide nanoparticles, (2014), *Int. J. Res. Eng. Technol* eISSN: 2319-1163 | pISSN: 2321-7308.
- [9] Rahdar A., Arbabi V., Ghanbari H., Study of Electro-Optical Properties of ZnS Nanoparticles Prepared by Colloidal Particles Method, (2012), *World Acad. Sci. Eng. Technol* 6(1), 214-216.
- [10] Shen X.S., Wang G.Z., Hong X., Zhu W., *Phys. Chem. Chem. Phys.* 11, 7450-7454 (2009); <https://doi.org/10.1039/b904712c>
- [11] Li C.C., Chang S.J., Su F.J., Lina S.W., Chou Y.C., *Physicochem. Eng. Aspects* 419, 209-215 (2013); <https://doi.org/10.1016/j.colsurfa.2012.11.077>
- [12] Rafiq M., Siddiqui H., Adil S.F., Assal M.E., Ali R., Al-Warthan A., *Asian J. Chem.* 25, 3405-3409 (2013); <https://doi.org/10.14233/ajchem.2013.13874>
- [13] Nguyen T.D., Do T.O., Size- and Shape-Controlled Synthesis of Monodisperse Metal Oxide and Mixed Oxide Nanocrystals, (2011), *InTech: Croatia*; <https://doi.org/10.5772/17054>
- [14] Song H.Y., Ko K.K., Lee B.T., Fabrication of silver nanoparticles and their antimicrobial mechanisms, (2006), *Eur. Cel. Mater* 11, 58-64.
- [15] Oluwafemi S.O., Revaprasadu N., A Facile, *Mater. Res. Soc. Symp. Proc.* 1138, 12-15 (2009); <https://doi.org/10.1557/PROC-1138-FF12-19>
- [16] Ravikumar S., Gokulakrishnan R., The Inhibitory Effect of Metal Oxide Nanoparticles against Poultry Pathogens, (2012), *Int. J. Pharm. Sci. Drug Res.* 4, 157.-159